

The power supply system model of the process submersible device with AC power transmission over the cable-rope

V M Rulevskiy¹, V G Bukreev², E O Kuleshova², E B Shandarova²,
S M Shandarov³ and Yu Z Vasilyeva²

¹ Research Institute of Automation and Electromechanics Tomsk State University of Control Systems and Radioelectronics, 53, Belinsky str., Tomsk, 634034, Russia

² Tomsk Polytechnic University, 30, Lenina ave., Tomsk, 634050, Russia

³ Tomsk State University of Control Systems and Radioelectronics, 40, Lenina ave., Tomsk, 634050, Russia

E-mail: bukreev@tpu.ru, shandarovaelena@mail.ru, kuleshova@tpu.ru

Abstract. A practical problem of power supply system modeling for the process submersible device with AC power transmission over the cable-rope was considered. The problem is highly relevant in developing and operation of submersible centrifugal pumps and submersibles. The results of modeling a symmetrical three-phase power supply system and their compliance with the real data are given at the paper. The obtained results in the mathematical and simulation models were similar.

1. Introduction

Nowadays, there is a problem of voltage regulation systems at the remote dynamic object [1-4]. Creating regulators of voltage assumes the use of synthesis methods of complex objects in modern control theory based on the description of dynamic processes in the variables state-space [5, 6]. To solve the problem, it is necessary to create a mathematical model that most accurately describes the operating modes of the object power supply system (PSS) and solves system differential equations [7, 8]. Various methods can be used to create a mathematical model [9]. At the primary stage of creating the mathematical model, it is assumed that the three-phase system is symmetrical. Thus, calculations can be performed only for one phase. Figure 1 shows the PSS scheme, reduced to a single phase. The pulse inverter connected to a DC power source with a nominal voltage of $U_s = 540$ V. A model with concentrated parameters was selected as a mathematical model of the cable line; see Figure 1 (cable). When the cable-rope length is 6 km, equivalent circuit parameters are as follows: active resistance - $R_{ak} = 19.2$ Ohm, inductance - $L_{ak} = 2.4$ mH, capacitance - $C_{ak} = 0.496$ uF.

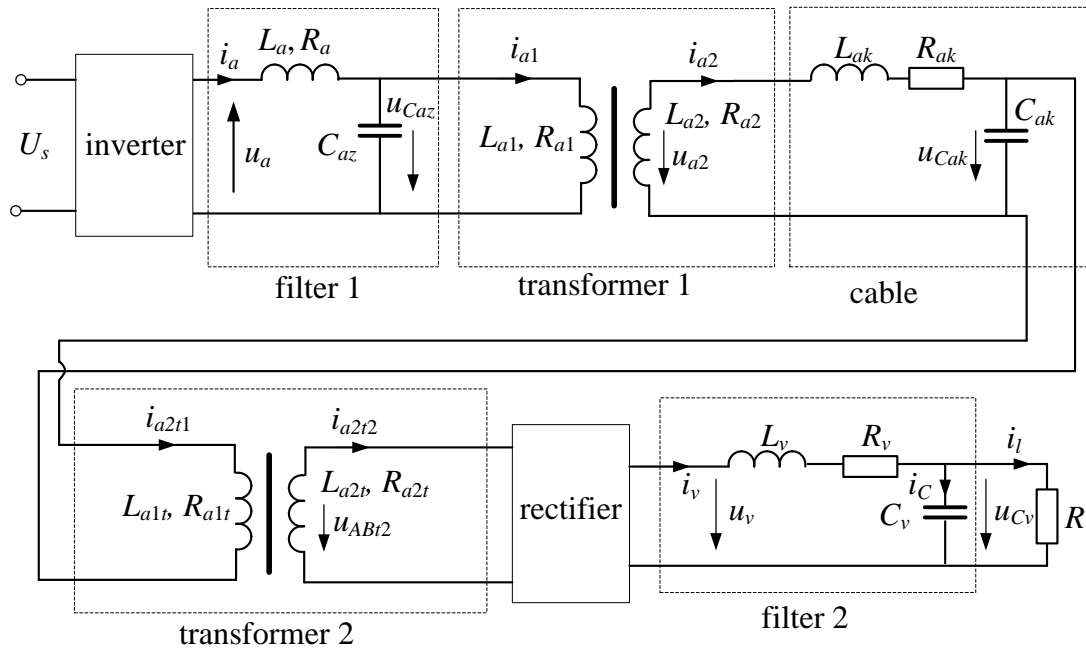


Figure 1. The power supply scheme, reduced to phase A.

The following parameters of the equivalent circuit are accepted:

1. For the input filter: $R_a = 1$ Ohm, $L_a = 0.4$ mH, $C_{az} = 6$ uF.
2. It should be noted that the special transformers were designed to operate in the considered power supply system. The parameters of these transformers, calculated from the results of short circuit and open circuit experiments, are shown in Table 1.

Table 1 . The transformers parameters

Step-up transformer (Fig.2, transformer 1)	
Rated power, windings voltage, frequency	$S_{n1} = 30$ kVA, $U_{n1} = 660$ V, $U_{n2} = 1830$ V, $f = 1000$ Hz
Winding connection	star-delta
Primary winding parameters	$R_{a1} = 0.866$ Ohm, $L_{a1} = 0.067$ mH
Secondary winding parameters	$R_{a2} = 2.28$ Ohm, $L_{a2} = 0.17$ mH
Magnetizing branch parameters	$R_{m1} = 494$ Ohm, $L_{m1} = 0.255$ H
Step-down transformer (Fig.2, transformer 2)	
Rated power, windings voltage, frequency	$S_{n2} = 60$ kVA, $U_{n1} = 1830$ V, $U_{n2} = 400$ V, $f = 1000$ Hz
Winding connection	delta-delta
Primary winding parameters	$R_{a1t} = 0.84$ Ohm, $L_{a1t} = 0.586$ mH
Secondary winding parameters	$R_{a2t} = 0.04$ Ohm, $L_{a2t} = 0.03$ mH
Magnetizing branch parameters	$R_{m2} = 373$ Ohm, $L_{m2} = 0.889$ H

2. Results of mathematical modeling

The rectifier (Figure 1, rectifier) is connected to the secondary winding of the step-down transformer (Figure 1, transformer 2) to obtain a constant load voltage.

Load parameters are calculated as a complex circuit impedance, $\underline{Z}_{eqv} = R_{eqv} + j\omega_v L_{eqv}$, at the fundamental frequency of the rectifier as a result of the equivalent second filter and the load on its

output. Active and reactive components of the complex impedance allow calculating the equivalent load parameters [10].

The power supply system, shown in Figure 1, is described by a system of differential equations in the Cauchy form [7, 8]. The mathematical model and the system of differential equations are given in ‘Mathematical model for power supply system of autonomous object with AC power transmission over cable-rope’.

Figure 2 shows plots of the input current after inverter $i_a(t)$ and currents of the primary $i_{a1}(t)$ and secondary $i_{a2}(t)$ winding of the first transformer. As we can see from the plots, the input filter considerably smooths ripple of the inverter current. A transient time is not more than one period.

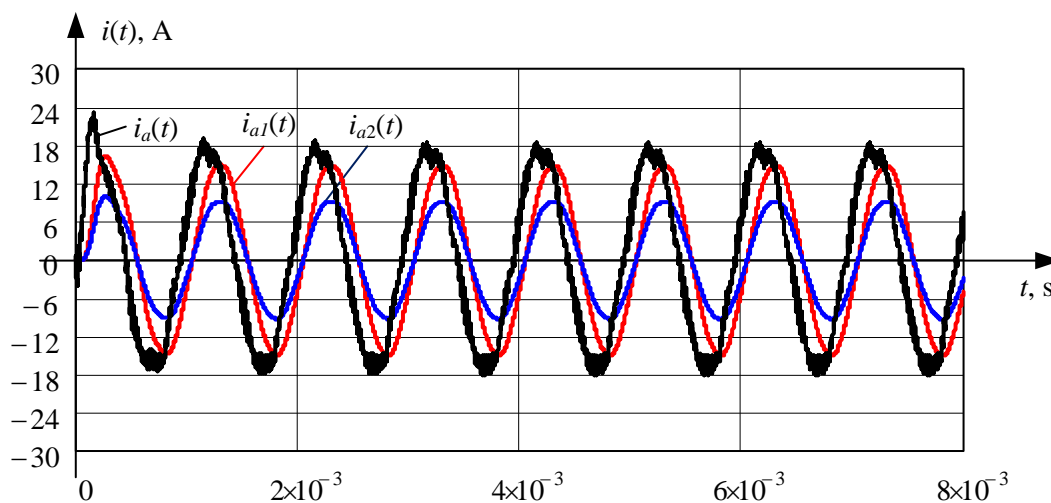


Figure 2. Input current $i_a(t)$ after inverter and linear currents of primary $i_{a1}(t)$ and secondary $i_{a2}(t)$ windings of transformer 1.

Primary u_{Ca2} and secondary u_{a2} phase voltage of transformer 1 are shown in Figure 3. The turn ratio is equal to $k_{f1}=0.624$.

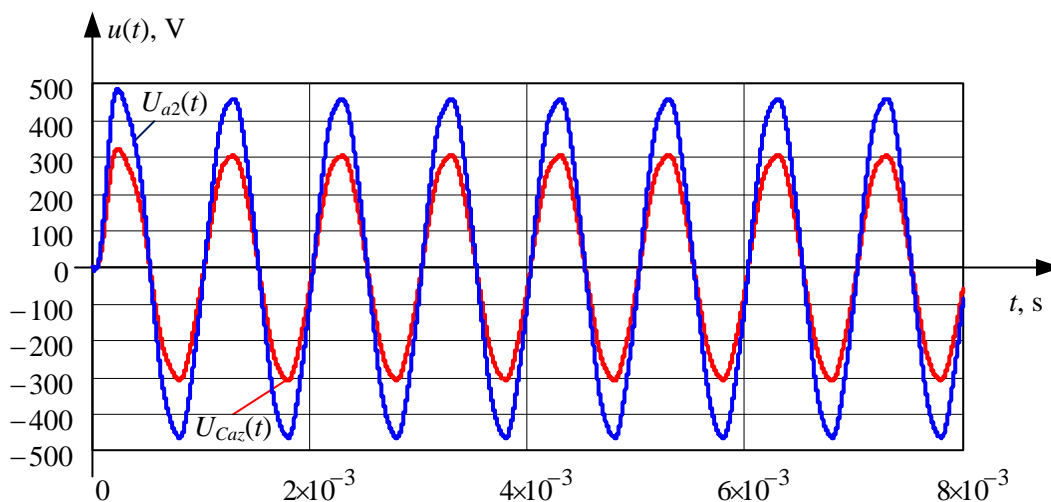


Figure 3. Primary and secondary phase voltage of transformer 1.

Figure 4 shows currents of the primary i_{a2r1} and secondary i_{a2r2} windings of transformer 2 with turn ratio $k_{f2} = U_{f2}/U_{f1} = 0.222$, where $U_{f1} = 925$ V is rated voltage of the primary winding, and $U_{f2} = 205$ V is rated voltage of the secondary winding. The currents have a harmonic form.

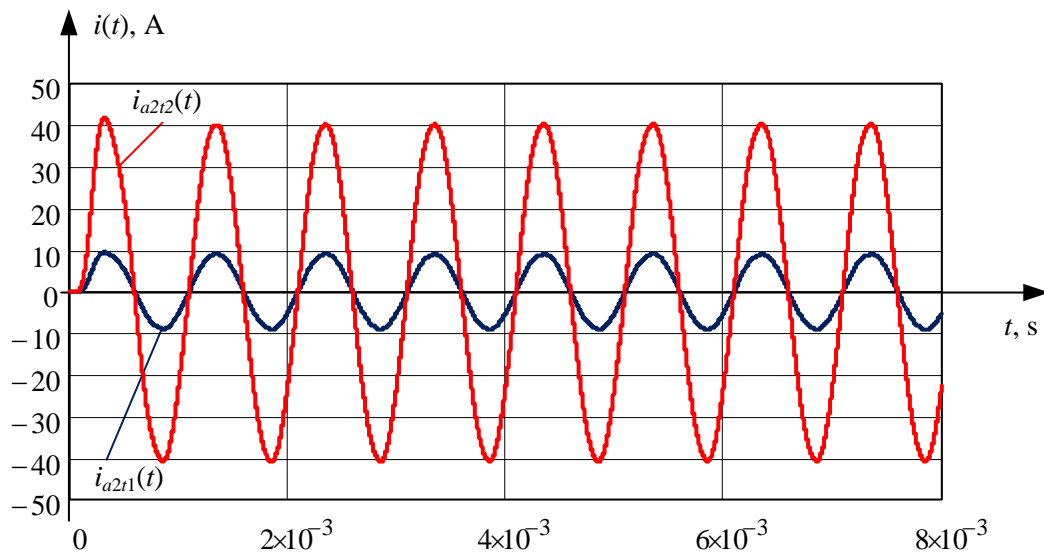


Figure 4. Currents of the primary i_{a2r1} and secondary i_{a2r2} windings of transformer 2.

Voltages on the primary and secondary windings of transformer 2 are different in turn ratio $k_{r2} = 0.222$. The voltage has a harmonic form.

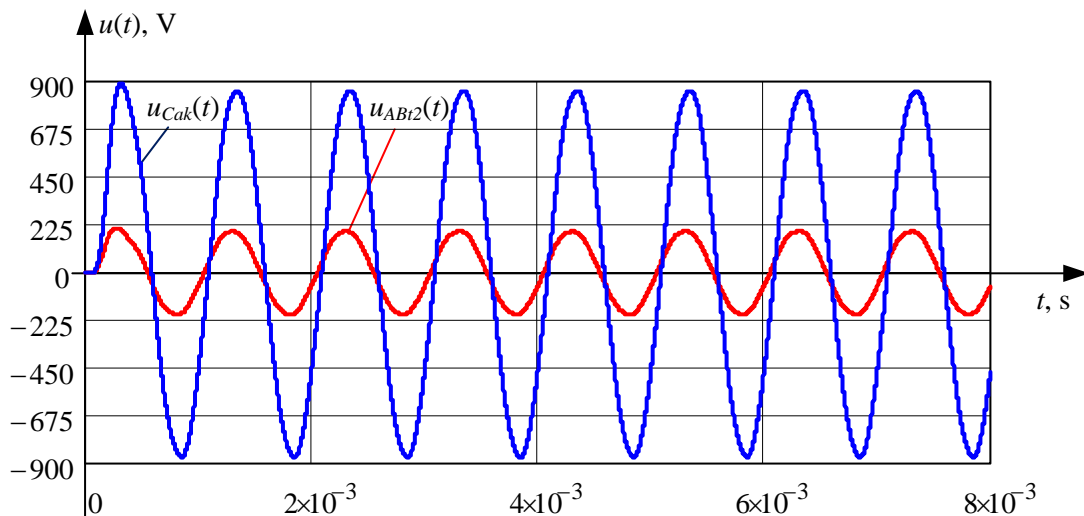


Figure 5. Voltage on the primary and secondary windings of transformer 2.

A transient process for currents i_d , i_C , i_{nag} is obtained due to the presence inductive and capacitive elements in the output filter. The transient process ends approximately at 0.12 s. The load current is equal to $i_{nag} = 69$ A in the steady-state mode. The capacity current approaches zero (Figure 6).

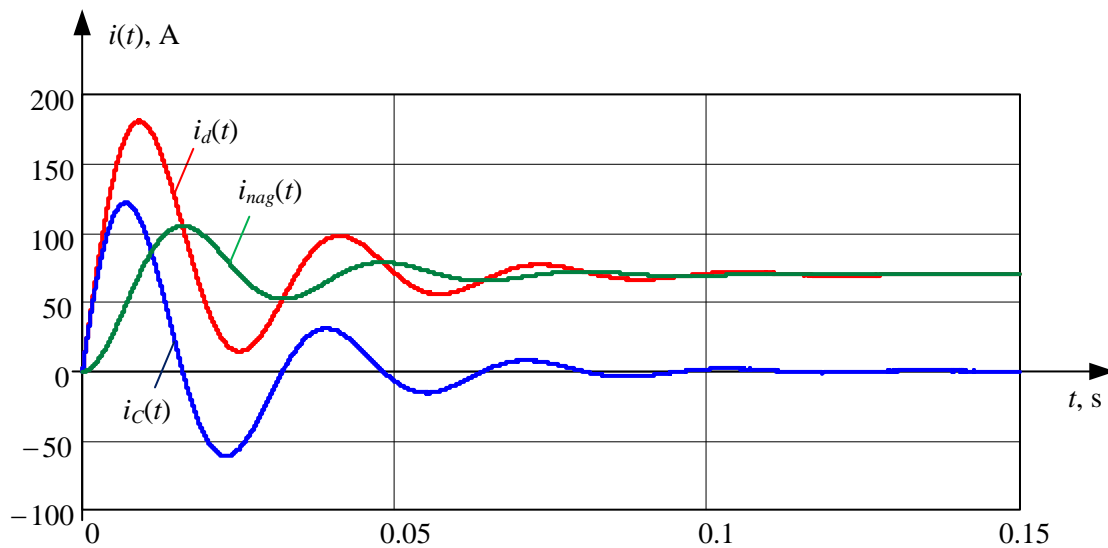


Figure 6. The current after rectifier i_d , filter capacity current i_c and load current i_{nag} .

Figure 7 shows the curve of the rectifier output voltage. As we can see from the figure, the rectified voltage has a six-phase ripple.

To smooth pulsations, the LC -filter is connected to the rectifier output. LC -filter parameters are: $R_v = 1 \text{ Ohm}$, $L_v = 10 \text{ mH}$, $C_v = 2240 \text{ uF}$. The PSS load is modeled by active resistance, which is accepted to be equal to $R = 4.7 \text{ Ohm}$ in the nominal operation mode.

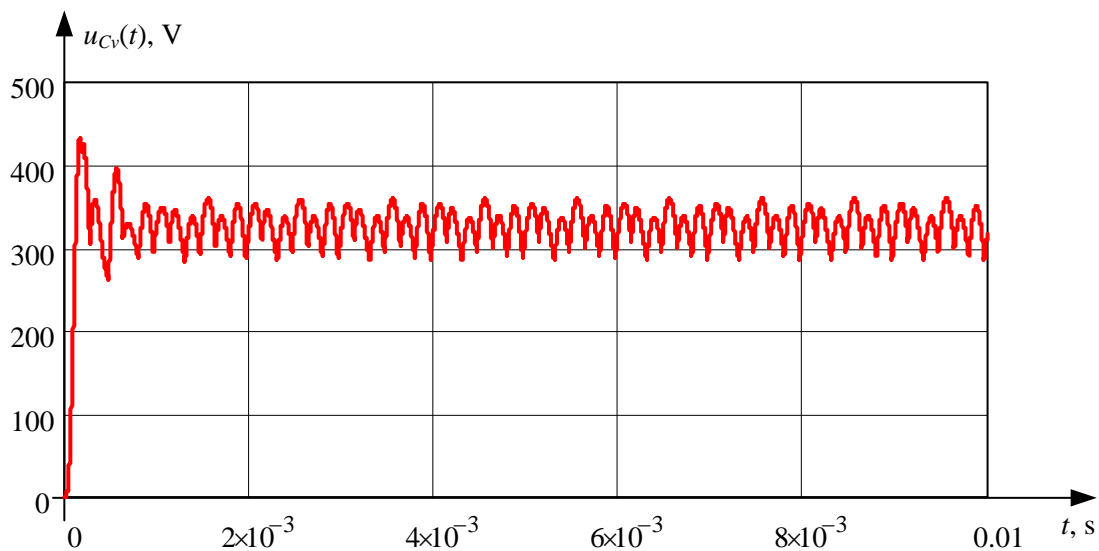


Figure 7. The curve of the rectifier output voltage.

There are smoothing pulsations after the filter. Experimentally, the voltage on the load of submersible device u_{os} was obtained by $329 \pm 1.5\%$ (Figure 8). The transient process ends at time $t=0.05\text{s}$.

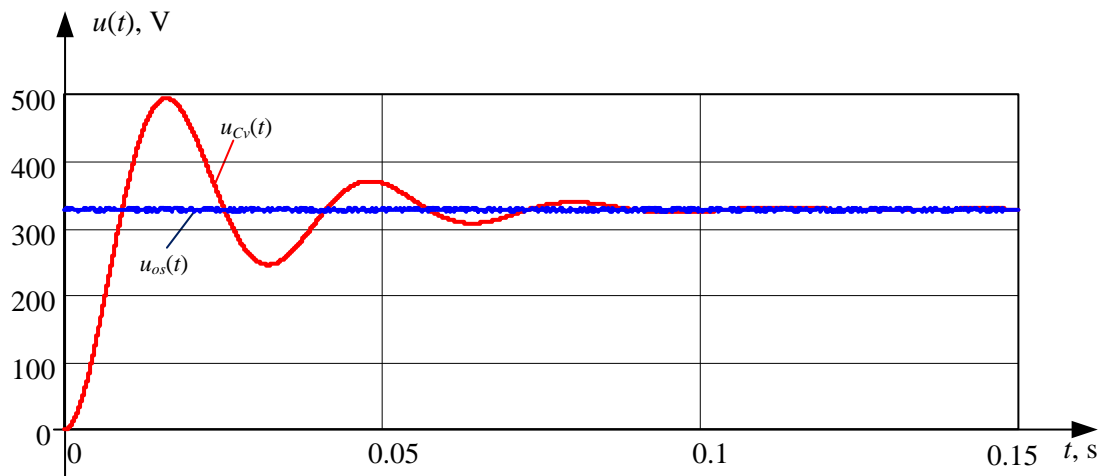


Figure 8. Calculated and experimental load voltage.

Figure 8 shows the plot of the voltage under load u_{Cv} . The voltage was obtained by mathematical modeling of the power supply system of the remote dynamic object. Power transmission is ensured by a cable-rope on alternating high frequency current. The mathematical model simulation was carried out in MathCAD software tools. The calculated results were compared with experimental results (Figure 8). The comparison showed that the difference in the steady-state mode is not more than 5%. Thus, these results confirm the adequacy of the developed model.

3. Conclusion

Thus, in this paper the mathematical model for the power supply system of the remote dynamic object with AC power transmission over the cable-rope was developed using MathCAD software tools. The calculated results were compared with experimental results.

The resulting mathematical model allows investigating static and dynamic modes of the power supply system of the submersible device.

On the basis of the resulting mathematical model, it is planned to develop an optimal control for the effective voltage stabilization under the load.

References

- [1] Xiang X, Niu Z, Lapierre L and Zuo M 2015 *HKIE Transact. Hong Kong Institution of Engineers* **22** 103-116
- [2] Song B, Zhang B, Jiang J 2016 *J. of Huazhong Univ. of Science and Techn.* **44**(7) 52-56
- [3] Maalouf D, Creuze V, Chemori A, Tamanaja I.T, Mercado E.C, Muñoz J.T, Lozano, R, Tempier O 2015 *Int. Journal of Advanced Robotic Systems* **12** 1-15
- [4] Cui R, Zhang X, Cui D 2016 *Ocean Engineering* **123** 45-54
- [5] Fang M-C, Hou C-S, Luo J-H 2007 *Ocean Engineering* **34**(8-9) 1275-1289
- [6] Shilin A A. and Bukreev V G 2014 *Thermal Eng.* **61** (10) 741-746
- [7] Mamis M S, Kaygusuzi A and Koksals M 2014 *Turk J Elec Eng & Comp Sci* **18**(1) 31-42
- [8] Kuleshova E O, Plyusnin A A, Shandarova E B, Tikhomirova O V 2016 *IOP Conf. Ser.: Mater. Sci. Eng. (Tomsk)* vol 124 (Bristol: IOP Publishing Ltd.) 012069
- [9] Goheen K R 1991 *J. of Robotic Systems* **8**(3) 295-317
- [10] Koran A, Labella T, Lai J-S 2014 *IEEE Transact. on Power Electr.* **29** 1285-1297